TRIBO-CORROSION BEHAVIOUR OF S-PHASE AGAINST S-PHASE TRIBOPAIRS[1]

Joseph Buhagiar[2]
Anne Jung[3]
Hanshan Dong[4]

Abstract

S-phase layers on austenitic stainless steels have demonstrated significantly enhanced wear and corrosion properties. Most of the tribocorrosion work on S-phase was conducted against an alumina or tungsten carbide counterpart. However, no work has been done on thecorrosion-wear behaviour of a tribopair both made from S-phase layers. However, S-phase against S-phase is both scientifically and technologically important since the S-phase can have commercial applications in the food and biomedical industries where there is a need of metal-on-metal sliding. In this work AISI 316 balls and discs were plasma surface alloyed with nitrogen and carbon to form S-phase layers and their corrosion-wear behaviour was tested in a 0.15M NaCl solution using a reciprocating wear tester. The results demonstrate that the S-phase tribopair can produce a markedly decrease in material lost when compared to an untreated tribopair.

Keywords: S-phase; Expanded austenite; Plasma nitriding; Plasma carburising; Plasma nitrocarburising; Corrosion-wear.

1 INTRODUCTION

Because of their excellent corrosion resistance, austenitic stainless steels are frequently used in corrosion-wear environments and find applications in the chemical, petrochemical, medical and food processing industries. For instance, austenitic stainless steels can be found as a main material in pumps, valves, bearing, fasteners and conveyor belts, where one contacting metal surface moves relative to the other.[1] However, austenitic stainless steels are characterized as having relatively poor wear mainly due to their low hardness and high adhesion tendency.

The low hardness and poor tribological properties of austenitic stainless steels was overcome in 1983, when Zhang and Bell[2] developed a low temperature plasma nitriding process to form a so called S-phase surface layer, which increases the hardness and wear resistance of austenitic stainless steels without any detriment to their corrosion resistance. Later work by Lewis et al.[3] showed that S phase can also be formed by low temperature carburising and in 2000 Blawert et al.[4] reported that plasma alloying with both nitrogen and carbon created a hybrid S-phase layer which inherited the advantages of both nitriding and carburising.

Thaiwatthana et al.[5] reported that both nitrogen and carbon rich S-phase can significantly improve the corrosion-wear resistance of austenitic stainless steel. Corrosion-wear experiments at Leeds University on S-phase coatings by Aldrich-Smith and Dearnley[6] have demonstrated that when using a WC-Co ball as counterface in 3%NaCl the S-phase coatings slightly improved the corrosion-wear resistance of the uncoated 316L stainless steel. However when rubbing against an alumina ball, S-phase coatings improved vastly the corrosion-wear resistance of the untreated 316L stainless steel. Clearly, the couterface has played an important role in determining the the corrosion-wear behaviour of S-phase layers.

It should also be indicated that in real applications it is very rare for stainless steel surfaces sliding against alumina ceramics or WC-Co cement. Indeed, there is ever-increasing demand for stainless steel against stainless steel. For example, metal-on-metal hip joints have been proved to be effective in reducing the wear debris from the metal-on-polymer hip joints. In addition, it has also been reported that S-phase surface tribopair can be used to reduce food contamination by rubber ring seal used in dosing pump against a stainless steel surface.[7]

To this end, corrosion-wear studies of a tribopair both made of S-phase layers were conducted in this work for the first time. Co-Cr ball against Co-Cr disc were used as the benchmark because Co-Cr based alloys have been successful used in metal-on-metal joint prostheses and in the chemical, petrochemical, medical and food processing industries.[8]

2 MATERIAL AND METHODS

2.1 Materials & Surface Treatments

The main material used in the present study was an AISI 316 austenitic stainless steel and its chemical composition is given in Table 1. This material was used in two forms: annealed bars (Ø25.4mm) and cold worked balls (Ø12.7mm).

Table 1. Material composition

| MATERIAL | Composition [wt%] | | | | | | | | | | | |
	Type	C	Si	Mn	P	S	Cr	Ni	Mo	N	W	Bal.
AISI 316	Bar spherel	0.08 max	1.0 max	2.0 max	0.045 max	0.03 max	16-18	10-14	2 -3	-	-	Fe
ASTM F75	Bar	0.35 max	1.0 max	1.0 max	0.02 max	0.01 max	26.5–30	0.5 max	4.5-7	0.25 max	1.0	Co
Stellite® 6	Ball	1.24	0.77	-	-	-	29.3	2.6	-	-	4.5	Co

From the annealed bar, disc samples of 6 mm in thickness were cut and one flat surface of the discs was wet ground using silicon carbide papers from 120 down to 1200 grit. The austenitic stainless steel balls (standard grade 100) were purchased from a commercial source without any sample preparation. The samples (discs and balls) were ultrasonically cleaned in acetone and dried with hot air prior to low temperature plasma surface alloying (LTPSA) to form the S-phase layers.

The samples, discs and balls, were placed in a specially designed jig, shown in Figure 1, and were subjected to three different LTPSA treatments: (i) with nitrogen (N430); (ii) with carbon (C500) and (iii) with both nitrogen and carbon (NC430). The process conditions (Table 2) were chosen based on our previous work, on the fact that a precipitate free S-phase can be formed on austenitic stainless steel by LTPSA under the same conditions.[9-11]

Following the surface treatments, all treated and untreated samples were polished using 6μm diamond paste for 5 minutes followed by a final polishing using 1μm diamond paste for another 5 minutes to remove the back-deposited superficial layer. The surface finish (Ra) of all the polished samples was between 0.06- 0.10μm.

Table 2. LTPSA process parameters

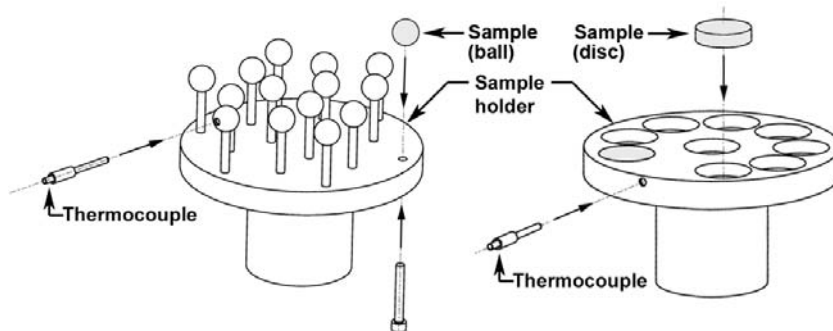| Code | Process Parameters | | | | Gas Mix [%] | | |
| | Furnace | Temperature | Time | Pressure | CH_4 | N_2 | H_2 |
	kW	[°C]	[hrs]	[Pa]			
N430	60	430	15	400	0	25	75
NC430	60	430	15	400	1.5	25	73.5
C500	40	500	15	400	1.5	0	98.5

Figure 1. Jigs for sample (ball and disc) treatment.

2.2 Materials Characterisation

Standard procedures were followed to prepare metallographic specimens to be examined under a Leitz DMRX optical microscope. This included cross-sectioning normal to the surface, mounting in phenolic resin, wet grinding with silicon carbide paper, polishing and etching in a solution containing 50ml of HCl (39% conc.), 25ml of HNO_3 (69% conc.) and 25ml of distilled water.

Surface hardness was measured using a Mitutoyo MVK-H1 micro-hardness tester with a Vickers indenter at a range of loads varying between 0.025 to 1kgf with three repeats for each measurement. A computer controlled Nano-Test 600 machine (Micromaterials, UK) was used to evaluate the surface hardness (H) of the as-received and plasma surface alloyed samples. The indentation tests were carried out normal to the surface and 15 points were selected in order to determine the values of H.

2.3 Reciprocating Wear Testing

Materials
Polished (Ra = 0,06 to 0.1µm) treated and untreated coupons were cut into blocks 5mm by 7mm by 6mm. The samples were then glued to another block and the treated surface was masked using tape. The assembly was then clamped into the holder and was spray lacquered. When the lacquer dried the masking tape was removed and the sample surface was cleaned with acetone.

In this test treated and untreated AISI 316 balls were used. Before testing the treated balls were slightly polished with ¼µm diamond paste and then washed in acetone whilst the untreated balls were used as supplied. During this test, the disc sample was made to move linearly against a stationary treated or untreated stainless steel ball of 12.7mm in diameter at an average speed of $12.5mms^{-1}$ (1Hz) for 200m in 0.15M NaCl solution. The normal contact load acting on the ball was of 39N and a wear scar of 6mm in length was produced. The test was repeated two times per condition. In order to compare the results against a tribopair which is well renowned for its excellent metal-on-metal corrosion-wear properties, a cast Co-Cr ASTM75 alloy disc was made to reciprocate against a powder metallurgy Co-Cr Stellite-6 ball was used as a benchmark. Their compositions can be found in Table 1.

Wear loss determination
The wear volume loss was determined by measuring the cross-section of a wear track using a stylus profilometer. To obtain the wear volume, the area of the wear scar was calculated using Simpson's rule and then multiplying by the length of the wear track. Three measurements were performed for each wear track and the average value is reported. The morphologies of the wear scars were characterised by a JEOL 7000 SEM with an EDX capability. The initial Hertzian contact pressures for the reciprocating-wear tests were calculated. The values obtained for the stainless tribopair and Co-Cr tribopairwas of 1.40GPa and 1.44GPa respectively.

3 RESULTS AND DISCUSSION

3.1 Microstructure

Discs
The cross-section microstructures shown in Figure 2 reveal the surface layer formed in the AISI 316 investigated. The surface modified layer in most treated

samples appears to be bright white. This is an indication that the surface layer has superior corrosion properties to the untreated material when etched. The distinct line at the substrate-layer interface, especially in the nitrided (Figure 2a) and carbonitrided (Figure 2b) layers and to a lesser extent in the carburised (Figure 2c) layers , is due to a grinding and polishing artefact where a step was formed by the difference in hardness between the hard S-phase layer and the soft substrate.
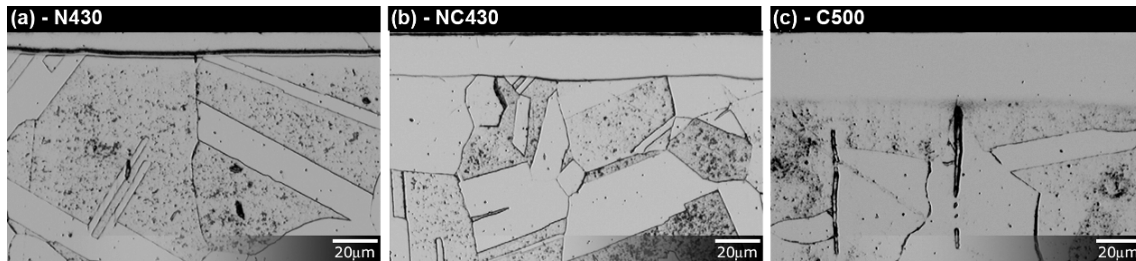

Figure 2. Microstructure of S-phase layers formed on AISI 316 discs.

Spheres

For the nitrided spheres at 430°C the S-phase layer formed (Figure 3a) is not completely white and this implies that there are some precipitates within it. Figure 3b shows the cross-section of a carbonitrided sphere and the S-phase layer is white in the bottom region and not completely white in the top-part. It is known that the whole S-phase case produced by hybrid carbonitriding consists of a top N-rich S-phase layer followed by a C- rich S-phase sublayer. This implies that this S-phase layer has precipitates in the nitrogen-rich part of the S-phase and is precipitate free in the carbon part of the S-phase. The carburised layer shown in Figure 3c on the other hand seems to be precipitate free.

Due to the hemispherical nature of the surface of the spheres it was impossible to conduct any further characterisation techniques (XRD, GDOES and hardness). The only proof that S-phase had formed in these spheres lies in the microscopical examination and hardness measurement.
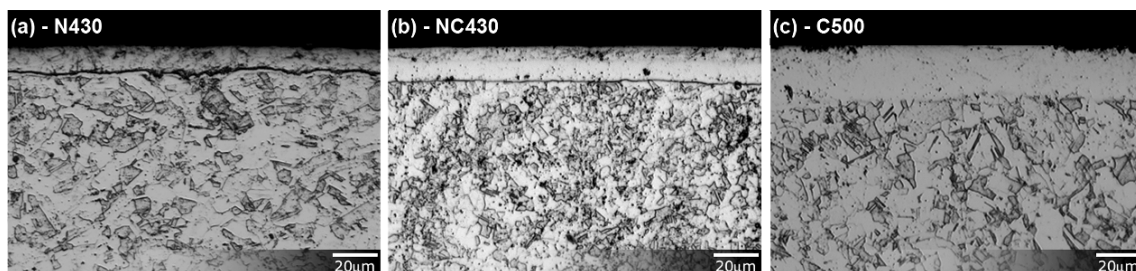

Figure 3. Microstructure of S-phase layers formed on AISI 316 balls.

3.2 Surface Mechanical Properties

Nano-hardness

Figure 4 summarizes the nano-indentation results for AISI 316 discs treated using three different processes. It can be clearly seen that this alloy can be hardened significantly using any of these surface alloying processes. The surface hardness decreased in the order of nitrided, carbonitrided and carburised layers.
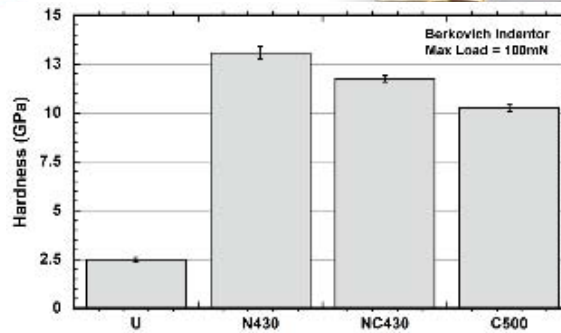
Figure 4. Nano-hardness of treated and untreated AISI 316 discs.

Surface hardness: load bearing capacity

Figure 5 shows the load bearing capacity of the AISI 316 disc treated using three different processes. The surface hardness of the nitrided specimen decreased quickly when the indentation load was above 100g, indication of its relatively low load bearing capacity. On the other hand, the 500°C carburised layer showed a lower surface hardness relative to the nitrided layer but the highest load-bearing capacity at higher loads. This is due to the fact that the carburised layer formed at 500°C is much thicker than the nitrided layer and therefore can support the indentation load better. With the strong support by the underlying C-enriched layer, the carbonitrided treated surfaces exhibited a much enhanced load bearing capacity as compared to the 430°C nitrided surface.
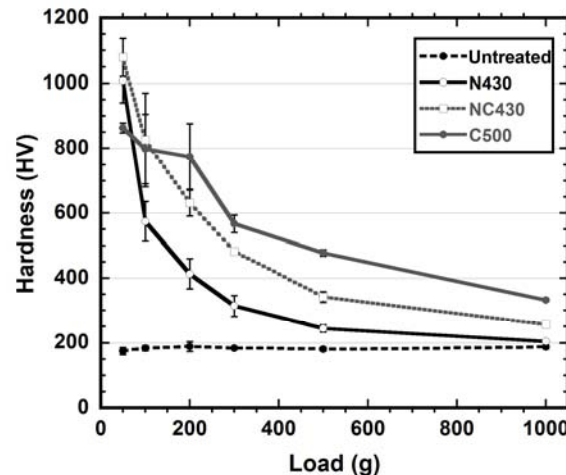

Figure 5. Surface micro-hardness at different loads of treated and ntreated AISI 316.

3.3 Corrosion-wear

3.3.1 Wear loss of discs

The wear loss of surface treated and untreated disc samples can be compared from Figure 6. The untreated discs sliding against treated balls showed poor wear resistance when compared to untreated AISI 316 discs sliding against untreated balls. The wear of the untreated discs is larger when reciprocating against C500 treated AISI 316 balls than N430 and NC430 treated ones although the latter are harder than the former. This seemingly abnormal wear can be explained by the fact that the wear of the treated ball can also occur and more wear was observed from C500 treated AISI 316 balls than N430 and NC430 treated ones. Accordingly, the damaged ball will in turn cause more wear to the counterpart disc.
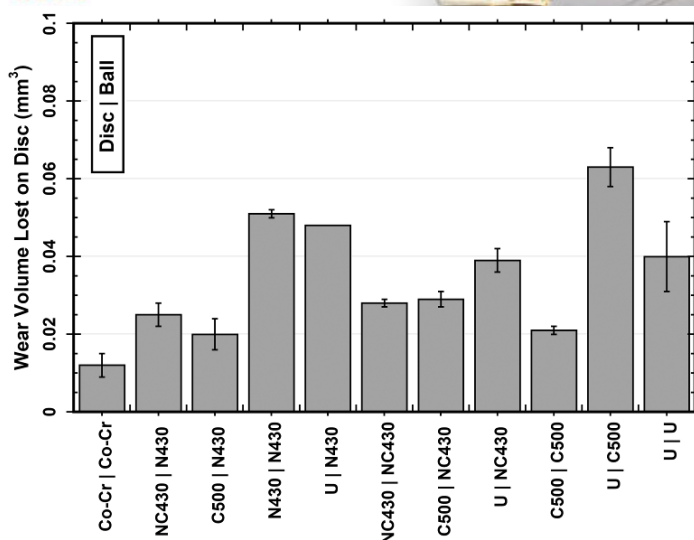
18th IFHTSE CONGRESS
International Federation for Heat Treatment and Surface Engineering
IFHTSE

ANAIS
PROCEEDINGS
ISSN 1516-392X

Figure 6. Wear volume loss of disc after reciprocating wear tests in 0.15M NaCl solution.

On the other hand, it was observed that most treated disc samples showed excellent wear resistance when sliding against treated balls. In fact some of the treated balls sliding against treated AISI 316 discs were comparable to the cobalt-chromium benchmark. The only exception was found in the nitrided ball against nitrided disc where they behaved very similarly to an untreated disc sliding against a nitrided ball. Due to this discrepancy further tests on untreated and nitrided tribo-pairs were conducted in both 0.15M NaCl solution and distilled water. The results are discussed in Section 3.3.4.

3.3.2 Wear of balls

The wear loss of the AISI316 balls sliding against AISI 316 discs treated by three different conditions is summarised in Figure 7. It can be clearly seen that the wear loss of the untreated ball was much larger when rubbing against the untreated discs than against the treated ones no matter what treatments were used. This could be partially attributed to the fact that the untreated balls and the discs have very similar metallurgical characteristics and thus high metallurgical compatibility. According to Rabinowicz's[12] adhesive wear theory, severe adhesive wear will occur because of the very large metallurgical compatibility between them. Secondly, as has discussed in Section 3.3.1, the untreated disc surfaces could be easily damaged through severe adhesive wear; the transferred materials will be work hardened by further rubbing, which causes more wear to the untreated ball.
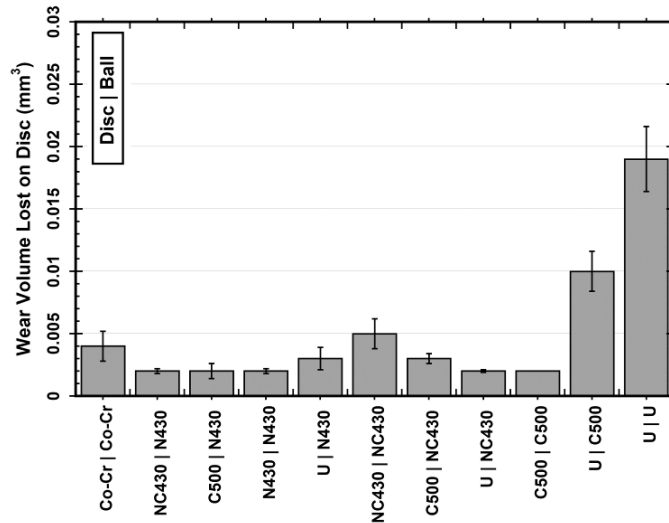
Figure 7. Wear volume loss of spheres after reciprocating wear tests in 0.15M NaCl solution.

In addition, it is also clear that all three plasma surface treatments, C500, N430 and NC430, can effectively improve the wear resistance of AISI316 balls sliding in 0.15M NaCl solution against AISI 316 discs. This is partially because of increased surface hardness (Figure 4) and thus the strong support (Figure 5) to the surface oxide film and partially because of the reduced metallurgical compatibility owing to the formation of S-phase layer.

3.3.3 Combined wear

The combined wear volume loss of the balls and discs together is illustrated in the stacked bar chart as shown in Figure 8. It was observed that for all the samples tested, whether they were surface treated or not, the wear of the AISI 316 balls is much less than that of the counterface discs, whether they are plasma treated or not. Also, larger wear occurred to the tribopair when one of the two surfaces was not plasma treated than the tribopair when both of the surfaces were treated with the exception of N430 treated AISI316 tribopair. It was also noticed that the combined wear of two plasma treated tribopairs (C500|N430 and C500|C500) is close to that of Co-Cr tribopair.
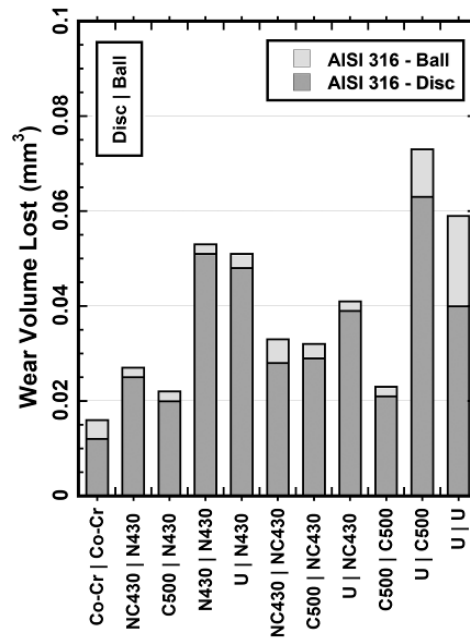
Figure 8. Combined wear volume loss of disc and spheres after reciprocating wear tests in 0.15M NaCl solution.

3.3.4 Effect of solution

It can be seen from Figure 9 that when tested in a 0.15M NaCl solution the wear loss of the nitrided AISI 316 disc against nitrided AISI 316 ball was larger than that of the untreated AISI 316 disc against untreated AISI 316 ball; however, when tested in distilled water, the wear of the disc in the nitrided tribopair was less than in the untreated tribopair. This demonstrates that the corrosion-wear of nitrided AISI 316 disc was governed more by corrosion effect than by the mechanical effect.
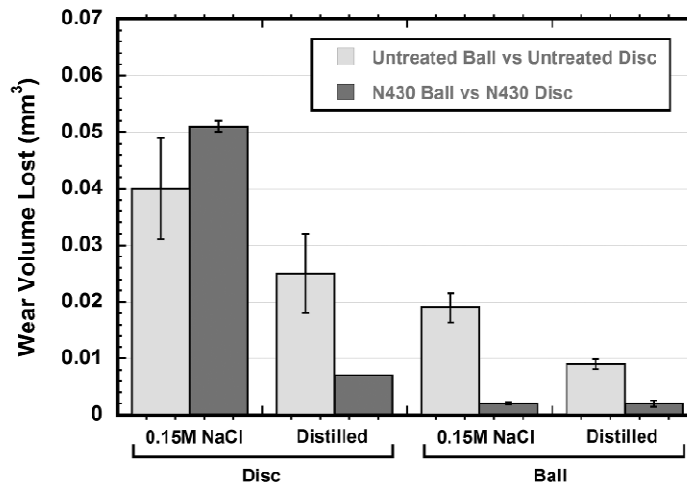

Figure 9. Wear volume loss of disc and spheres after reciprocating wear tests in distilled water and 0.15M NaCl solution.

For the untreated balls, the corrosion-wear in 0.15M NaCl solution was almost the same as in distilled water. This implies that the corrosion-wear of the untreated ball was dominated by the mechanical effect. On the other hand, the corrosion-wear of the nitrided ball was larger in 0.15M NaCl solution than in the distilled water. Therefore, corrosion effect may have played an important role in the corrosion-wear of the nitrided ball.

Wear morphologies of untreated AISI 316 tribopair

Figure 10a shows typical corrosion-wear morphologies of untreated AISI 316 disc after rubbing the untreated AISI 316 ball in 0.15M NaCl solution. Severe adhesion tearing, deep grooves in the direction of motion together with corrosion attack were observed in the middle of the wear track. EDX analysis has also revealed a high presence of oxygen within the wear track. Therefore, the possible mechanisms governing the wear of untreated AISI 316 tribopair were abrasive, adhesive and oxidative. The wear morphologies of the untreated AISI 316 disc against the untreated ball formed in distilled water in general seems similar to the one formed in 0.15M NaCl solution (Figure 10b). It can be found by comparing Figure 10a with Figure 10b that although adhesive and abrasive wear are still the major wear mechanism the wear track had less corrosion attack and appeared to be smoother.
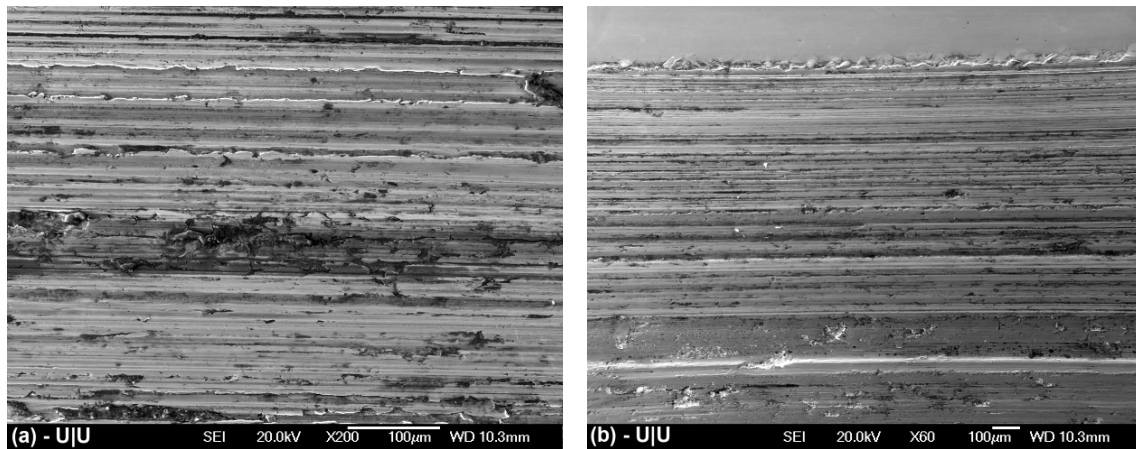

Figure 10. SEM images of untreated AISI 316 versus untreated AISI 316 in (a) 0.15M NaCl Solution and (b) distilled water.

This is mainly because the untreated austenitic stainless steel discs are very soft and ductile. Therefore, the surface oxide films on the untreated austenitic stainless steels tribo-pairs will easily break down under the mechanical interaction due to the lack of the necessary mechanical support from the substrate. This leads to direct rubbing of metal-against-metal, which in turns creates adhesion of the asperities of the two rubbing faces. Because austenitic stainless steels are very ductile, growth of adhesive junctions is fast, thus giving rise to material transfer and severe adhesive wear of the untreated surfaces. Work hardening of the transferred material to the counterpart ball will occur during the sliding process due to the low stack fault energy and strong work hardening tendency of austenitic stainless steels. These hardened transferred materials will abrade the soft disc, thus leading to abrasive wear .

Wear morphologies of nitrided AISI 316 tribopair

The wear track for nitrided tribopair is characterised by abrasive wear. Figure 11a reveals parallel grooves in the direction of sliding which are characteristics for abrasive wear. EDX analyses, has revealed that no oxygen was detected within the wear track. This change in mechanisms from the untreated to treated tribopair is attributed to the strong mechanical support from hardened S-phase layer to the surface passive film, which could avoid direct metal-on-metal contact in stainless steel tribo-pairs.
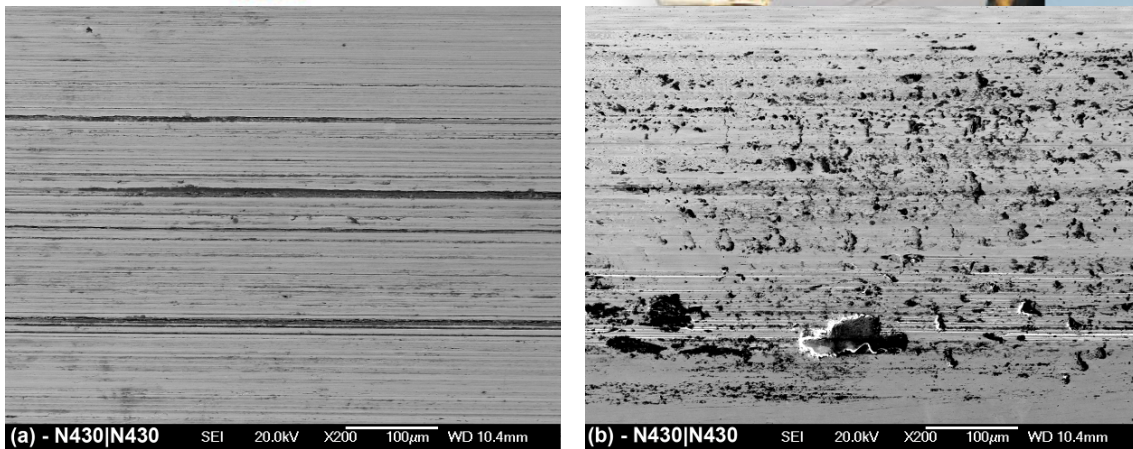
Figure 11. SEM images of nitrided AISI 316 versus nitrided AISI 316 in (a) 0.15M NaCl Solution and (b) distilled water.

The wear track produced in distilled water, shown in Figure 11b, shows mild abrasive wear and EDX analysis revealed that the dark areas are rich in oxygen. The kind of wear on this track is less severe than that observed in 0.15M NaCl solution and this explains why the wear volume loss (Figure 9) is much lower.

5 CONCLUSIONS

• All three plasma surface treatments, C500, N430 and NC430, can effectively improve the wear resistance of AISI316 balls sliding in 0.15M NaCl solution against AISI 316 discs. This is partially because of increased surface hardness and thus a strong support to the surface oxide film.

• The combined wear of S-phase against S-phase for the two sample pair C500|N430 and C500|C500 is close to that of the Cobalt-based tribopair under reciprocating sliding wear conditions in 0.15M NaCl solution at a maximum contact pressure of about 1.4GPa.

• S-phase surface engineering of austenitic stainless steels makes it possible for austenitic stainless steel to slide against austenitic stainless steel without causing scuffing or seizure. Therefore hardened austenitic stainless steels can compete against more expensive alloys, such as cobalt-based alloys, in wear applications such as that found in the food, pharmaceutical and biomedical industries.

Acknowledgements

REFERENCES

1   J.R. Davis (Ed.) *Stainless Steels*. ASM International, Ohio. 1994.
2   Z.L. Zhang, T. Bell. *Structure and corrosion resistance of plasma-nitrided AISI 316 Stainless Steel*. in: T. Bell (Eds.), *Third International Congress on Heat Treatment of Materials*, The Metals Society, 1983, pp.

3   D.B. Lewis, A. Leyland, P.R. Stevenson, J. Cawley, A. Matthews, Surface & Coatings Technology 60 (1993) 416-423.
4   C. Blawert, B.L. Mordike, G.A. Collins, K.T. Short, Y. Jiraskova, O. Schneeweiss, V. Perina, Surface & Coatings Technology 128-129 (2000) 219-225.
5   S. Thaiwatthana, X.Y. Li, H. Dong, T. Bell, Surf. Eng. 19 (2003) 211-216.
6   P.A. Dearnley, G. Aldrich-Smith, Wear 256 (2004) 491-499.
7   H. Dong, International Materials Review 55 (2010) 65-98.
8   J. Chen, X.Y. Li, T. Bell, H. Dong, Wear 264 (2008) 157-165.
9   X.Y. Li, J. Buhagiar, H. Dong, Surf. Eng. 26 (2010) 72-78.
10   J.P. Buhagiar, H. Dong, Key. Eng. Mat. 373-374 (2008) 296-299.
11   J. Buhagiar, X.Y. Li, H. Dong, Surf. Coat Technol. 204 (2009) 330-335.
12   K.C. Ludema, *Friction, Wear, Lubrication A Textbook in Tribology,.* CRC Press, Washington DC, 1996.